Effect of a Low-Dielectric Interior on DNA Electrostatic Response to Twisting and Bending

A. G. Cherstvy

Max-Planck-Institut für Physik komplexer Systeme, Nöthnitzer Strasse 38, 01187 Dresden, Germany, and Institut für Festkörperforschung, Forschungszentrum Jülich, D-52425 Jülich, Germany

Received: May 30, 2007; In Final Form: August 14, 2007

We study the effects of a low-dielectric core of rod-like macromolecules on their electrostatic persistence lengths. We use the exact solution of the linear Poisson−Boltzmann equation for the potential of a charge on the surface of a low-dielectric cylinder. We apply the results to the B-DNA molecule, modeled as a double helical array of discrete charges wound on the surface of a low-dielectric rod. For this charge geometry, we calculate the change in the electrostatic twist persistence as compared to DNA with a water-permeable core. We also discuss possible effects of the low-dielectric molecular core on DNA bending persistence.

1. Introduction

The calculation of the electrostatic persistence length (PL) of polyelectrolytes is a long-standing problem. The problem originated from the Odijk−Skolnick−Fixman (OSF) theory for the bending PL of a long linear array of charges in the near-the-rod limit.[1] This is the simplest theory that can account for the electrostatic contribution to the DNA bending PL. It is based on summation of the Debye−Hückel (DH) potentials acting between the charges on the chain in an electrolyte solution

$$\Psi_{DH}(z) = l_B e^{-\kappa z}/z \tag{1}$$

Here, $l_B = e_0^2/(\epsilon k_B T)$ is the Bjerrum length (∼7 Å in water), and $1/\kappa = 1/\sqrt{8\pi l_B n_0}$ is the Debye screening length in a 1:1 electrolyte solution with the concentration of a monovalent salt of n_0. The linear DH potential results in a low salt limit in a quadratic dependence of the electrostatic bending PL of weakly bent polyelectrolytes on the screening length in solution,[1] namely

$$l_{p,DH}^{el} = l_B/(4\kappa^2 b^2) \tag{2}$$

where b is the average separation between the charges on the chain. In the limit of low salt, the electrostatic contribution to the DNA bending PL can exceed the mechanical DNA PL that is equal to about 500 Å. The OSF theory has been modified, in particular, for the finite length rods;[2] the end effects of the polyelectrolyte have also been treated.[3] For flexible polyelectrolytes, in contrast to the weakly bent semiflexible ones, the charge−charge interactions result in more subtle effects on the chain electrostatic persistence; see, for example, ref 4.

The OSF theory has been successfully applied to the description of many polyelectrolyte properties of DNA; for examples, see ref 5. It neglects, however, such important ingredients of DNA structure as the low-dielectric DNA core and the helicity of DNA charges. More advanced theoretical models have been suggested in the literature to treat the effects of the DNA helical charge pattern both on electrostatic DNA bending[6] and twisting[7,8] PLs. For instance, the bending PL of a helical DNA molecule was recently shown[6] to be very close to the OSF result calculated at the same polyelectrolyte axial charge density. All of these models however use the linear DH potentials, without considering a low-dielectric permittivity of the DNA interior.

Some modifications of the OSF theory exist for the case of an electrolyte-impermeable cylinder interior as well. The analytical treatment of charge−charge interactions on the surface of a low-dielectric torus is, however, a complicated mathematical problem. A numerical solution of the nonlinear Poisson−Boltzmann equation for a low-dielectric torus in an electrolyte solution has been presented by Le Bret.[9] It was shown that for a uniformly charged torus with DNA-relevant parameters, the bending PL is dramatically larger than the OSF results at moderate and large ionic strengths, $n_0 > 0.01$ M, and l_p^{el} is quite close to the OSF prediction at low ionic strengths, $n_0 < 0.001$ M. In the OSF theory for DNA, the final value of the Manning charge parameter ξ[10] was set to unity in this model, that is, $b = l_B$. It is done in order to account for the condensation of counterions onto highly charged polyelectrolytes. In the weak screening regime, the calculated l_p^{el} was shown to scale with κ similar to the OSF results, whereas at high n_0, it revealed a $l_p^{el} \propto \kappa^{-0.5}$ scaling behavior. These results were shown to describe the experimental data of Hagerman[11] on DNA bending PL much better than the original OSF predictions. Very similar results for l_p^{el} have been obtained from the linear Poisson−Boltzmann theory by Fixman[12] in the framework of expansion of the electrostatic potential of a bent rod in higher powers of the rod curvature (for comparison, see Figure 2 in ref 9 and Table 3 in ref 12). In both of these models, the number of charges per unit surface element was kept constant upon the rod deformations (no charge rearrangements).

Recently, the problem of $l_p^{el}(\kappa)$ dependence for rigid polyelectrolytes has been revisited using an approximate analytical solution of the linear Poisson−Boltzmann equation for the potential of a uniformly charged torus immersed in electrolyte solution.[13] In particular, a strong $l_p^{el}(\kappa)$ dependence has been revealed for different regimes of charge density variations along the toroidal circumference upon rod cyclization. In particular, in the high salt limit, the scaling of $l_p^{el}(\kappa)$ can vary between $l_p^{el} \propto \kappa^{-3}$ for a constant surface charge density of the torus and $l_p^{el} \propto \kappa^{-1}$ for a constant number of charges per unit area on the torus surface (like in the Le Bret and Fixman calculations).

10.1021/jp074166z CCC: $37.00
Published on Web 10/17/2007

The OSF scaling $l_p^{el}(\kappa) \propto \kappa^{-2}$ has been obtained in this theory for some "intermediate" surface charge density variations. For all charge variations on the torus surface considered, the OSF limit was recovered as the small radius of the toroid goes down. It was claimed that the OSF theory strongly overestimates the rod bending PL at low salt. A possible reason for that is the fact that the summation is performed in the OSF model over an infinite number of charges along the chain contour, while the torus contains a finite number of charges. The OSF theory however underestimates l_p^{el} at larger salinities as compared to the solution for a torus with no charge rearrangement, presumably because of the compression of charges on the inner torus surface; see Figure 5 in ref 13.

The DNA twist PL, l_{tw}^{el}, has been calculated for the case of a water-filled helical array of charges in ref 7. An estimation of 40−50 Å at a physiological salt concentration of $n_0 \approx 0.1$ M has been suggested for l_{tw}^{el}, with only a weak dependence on the actual salt amount in solution. This value gives a relatively small fraction of the total DNA twist PL, which appears to be about 750 Å. Some simple analytical expressions in the limit of thin helices have also been obtained for DNA twist persistence in ref 8. In these two papers, in particular, it was shown that DNA twist PL l_{tw}^{el} can change sign, depending on the parameters of the helix and salt conditions.

The purpose of this paper is to understand the implications that a DNA low-dielectric core has on DNA twisting and bending PLs. We do not consider here the case of multivalent salts, which interact much stronger with DNA and thereby induce considerable deformations of the DNA molecular structure being adsorbed onto the molecule. There are several theoretical models about spontaneous DNA bending upon binding of small multivalent cations.[14] We use the analytical solution for the potential Ψ of a point charge on the surface of a low-dielectric straight rod, first obtained by Fixman and Skolnick (FS) in ref 15. Although we use below the known analytical results, their implications and the magnitude of the effects on DNA twist and bend PLs for realistic DNA parameters has not been studied, to the best of our knowledge.

2. Model, Approximations, and Basic Equations

The solution of the Poisson−Boltzmann equation predicts[15] that due to a low-dielectric rod interior, the interaction of two electric charges on the same side of the rod is enhanced while that on the opposite rod side is diminished, as compared to the DH potential Ψ_{DH}. The reason for that is as follows. The lines of the electric field originating on the charge avoid passing through the low-dielectric rod interior. Thus, the screening of two charges on the opposite sides of the rod requires an "embracing" of the rod surface by the electric lines. Longer distances in the electrolyte required for this path result in weaker electrostatic interactions between the charges.[15] For two charges on the same side of the rod, the electric field lines are expelled from the rod core. Thus, effectively, a part of space occupied by the rod is ineffective in screening. The electric lines concentrate in the remaining electrolyte solution, producing less effective screening of charges and thus higher interaction energies. Similar enhancement of the electrostatic potential also takes place near a low-dielectric half-space[16,17] and near a low-dielectric sphere[18,19] immersed in electrolyte solution.

We consider a DNA core as a rod-like piece of homogeneous and continuous dielectric with a low permittivity ϵ_c immersed in aqueous solution with a high dielectric constant ϵ. One can argue, of course, whether such a model is applicable to describe real DNA, with the diameter of only about 20 Å and with a grooved structure. Also, a sharp dielectric contrast boundary we use below might be smeared out in the vicinity of a highly charged DNA surface. Namely, near the DNA surface, the dielectric constant is likely to be lower than that in the bulk water due to the structuring of dipolar water molecules. This might further enhance the electrostatic interactions of charges close to the DNA surface, as compared to those calculated below within a model with a jump of dielectric constant on the rod surface. Also, we assume that the charges are positioned right at the dielectric boundary. The position of charges with respect to this boundary is, however, known to have a dramatic effect on the electrostatic self and interaction energy of the charge distribution, similar to the electrostatic properties of globular proteins.[20] We model DNA as a double helix with 10 "base pairs" per helical turn. Every base pair contains two charges (which represent the charges of DNA phosphates) positioned on the opposite sides of the rod. The twist angle between the base pairs is $\beta_{DNA} = 2\pi/10$, while the width of the minor and major DNA grooves are assumed, for simplicity, to be equal to π.

For clarity, we avoid below a detailed consideration of counterions condensed on the DNA. It is however well-known that the condensation of counterions on highly charged DNA molecules with $\xi = l_B/b \approx 4.2 > 1$ takes place very effectively,[10] both into the DNA grooves and onto the DNA phosphate strands. The actual positions of the counterion binding sites depend on the cation's valency and its chemical preference to some sites on DNA; see, for example, ref 21. The Manning theory predicts that in the low salt limit, the fraction of the DNA charge neutralized by the condensed counterions is $1 - 1/\xi \approx 0.76$ in solutions of monovalent salts. This fraction approaches $1 - 1/(2\xi) \approx 0.88$ in the case of divalent counterions.[10,22,23] If the counterion condensation were taken into account in our model, the charge of the DNA phosphates would be effectively diminished down to about $1/\xi$ of its original value in 1:1 salt solutions. The strength of electrostatic interactions and thus the PLs are then decreased by about 20 times, being proportional to the product of electric charges. This is, however, a very rough estimate, which might be valid in the low salt limit only.

At physiological salt concentrations, however, the fraction of cations condensed onto DNA can be smaller than that of the predictions of the Manning theory in the low salt limit, particularly due to a weaker electrostatic binding energy of cations to the DNA (see ref 22, where the Manning theory of counterion condensation onto the planar surface, rod, and sphere has been revisited for finite but still small salt amounts; see ref 23, where the discussion of Schurr and Manning's theories of counterion condensation at elevated salt concentrations is presented; see also ref 21, where some isotherms of counterion adsorption onto the DNA are discussed). On the other hand, adsorption of cations onto DNA can be enhanced due to higher salt amounts in the bulk. Note that the degree of counterion condensation can also differ for a low-dielectric and water-filled rods (through ion self-energy) and thus can affect the PLs calculated below in a nontrivial fashion at different salt amounts. This is, however, a separate problem, and below, we skip the consideration of cation condensation effects onto low-dielectric helical DNA altogether.

The dimensionless potential Ψ created by a unit point-like charge e_0 positioned at the distance $r \geq a$ from the axis of a low-dielectric rod follows from the solution of the linear Poisson−Boltzmann equation obtained in ref 15

$$\Psi(\varphi,z,r) = \int_0^\infty dk\tilde{\Psi}(0,k,r)2\cos(kz) + \sum_{m=1}^{\infty} 2\cos(m\varphi)\int_0^\infty dk\tilde{\Psi}(m,k,r)2\cos(kz) \quad (3)$$

where

$$\tilde{\Psi}(m,k,r) = -\frac{l_B\epsilon}{\pi a}\frac{I_m(\kappa_k^c a)K_m(\kappa_k r)}{\epsilon\kappa_k I_m(\kappa_k^c a)K_m'(\kappa_k a) - \epsilon_c\kappa_k^c K_m(\kappa_k a)I_m'(\kappa_k^c a)} \quad (4)$$

Here, z is the distance from the charge along the rod axis, and φ is the azimuthal angle in cylindrical coordinates; $\kappa_k = \sqrt{\kappa^2+k^2}$ and $\kappa_k^c = \sqrt{\kappa^{c2}+k^2}$ are the modified screening lengths in an electrolyte solution ($r > a$) and inside of the rod ($r < a$); $I_m(x)$ and $K_m(x)$ are the modified Bessel functions of the second kind. Further, for simplicity, we set to zero the concentration of mobile ions inside of the cylinder core, that is, $\kappa^c = 0$. The convergence of series over m in eq 3 is quite slow, especially for small z and for larger values of κ. The values $\varphi = 0$ and $\varphi = \pi$ are related to the potential on the same and on the opposite side of the rod, correspondingly.

3. Results for the Double Helix

3.1. Twisting. The $\Psi(z)$ dependence calculated at $r = a$ and for φ values corresponding to positions of phosphate charges on B-DNA for two different κ values is presented in Figure 1. We observe that the interaction energy $k_BT\Psi(z)$ of two charges situated on the same side of the rod is enhanced, while the interaction is impeded for charges on the opposite sides of the rod, as compared to the DH potential. Naturally, for smaller rod radii a, the enhancement effect originating from the rod low-dielectric core is diminished because the charges interact more effectively through the electrolyte solution; see Figure 2.

The electrostatic part of the DNA twist rigidity l_{tw}^{el} is the second derivative of the interaction energy of charges $E_{el}(\beta)$ in the double helical structure over the twist angle between the nearest DNA base pairs, β, calculated at $\beta = \beta_{DNA}$. This definition implies that β varies along the whole helix. The value of l_{tw}^{el} provides some characteristic length scale for the static response of the DNA duplex to twisting. The real DNA twist PL, being defined as a statistical quantity describing the decay of directional correlations along the DNA chain in solution, appears to be twice as large as our characteristic twist rigidity length l_{tw}^{el}.[24,25] We thank an anonymous referee for bringing this point to our attention.

We have calculated the electrostatic energy of the double helix with 10 base pairs per turn as a function of the twist angle between the neighboring base pairs β. We have summed the pairwise interactions between the changes in the helix both for the DH and FS potentials twisting the whole helix. The energy at typical values of the screening length has a pronounced maximum at $\beta = 0$ (the linear array of charges with effectively infinite helical pitch H) and a smaller maximum at $\beta = \pi/2$. The energy of the helix is higher and the maxima are more pronounced for the case of a low-dielectric rod. The maxima correspond to unstable molecular configurations and to negative values of the twist PL. For the values of β relevant for real DNA molecules, the l_{tw}^{el} is typically positive. The energy shape is symmetric with respect to $\beta = \pi$.

The results for l_{tw}^{el} obtained from the summation of the DH and FS potentials are shown in Figure 3. The same number of charges is taken in the summation for both cases. The dependence of l_{tw}^{el} on κ is quite similar for both potentials. For the low-dielectric rod, the l_{tw}^{el} values are, however, larger due to the enhanced interactions of closely positioned charges along the rod surface. In general, the l_{tw}^{el} reveals a much weaker dependence on $1/\kappa$ than that for the electrostatic bending PL, eq 2. An explanation for this could be that, contrary to DNA bending, DNA twisting does not change the separations between the charges considerably.

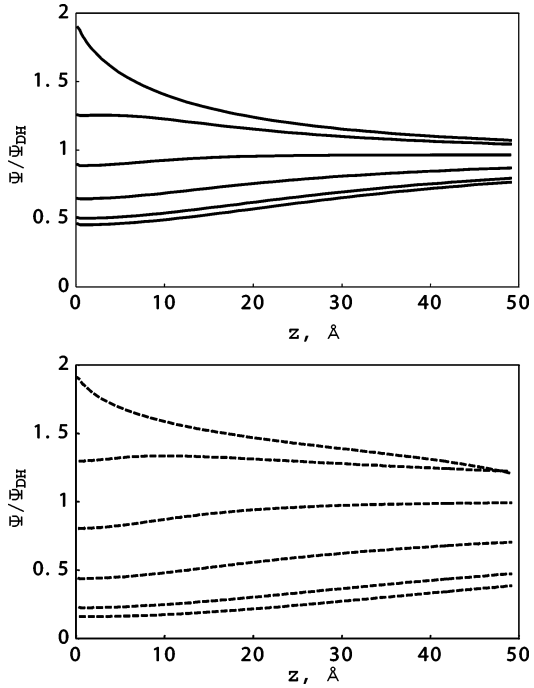

Figure 1. The electrostatic potential of a point charge (eq 3) along the surface of a low-dielectric rod z for the azimuthal angles $\varphi = 0$, $\pi/5$, $2\pi/5$, $3\pi/5$, $4\pi/5$, and π (the curves from top to bottom). Dotted curves correspond to $\kappa^{-1} = 10$ Å, and solid curves are plotted at $\kappa^{-1} = 100$ Å. Parameters: $\epsilon_c = 2$, $\kappa_c = 0$, $\epsilon = 80$, $a = 10$ Å.

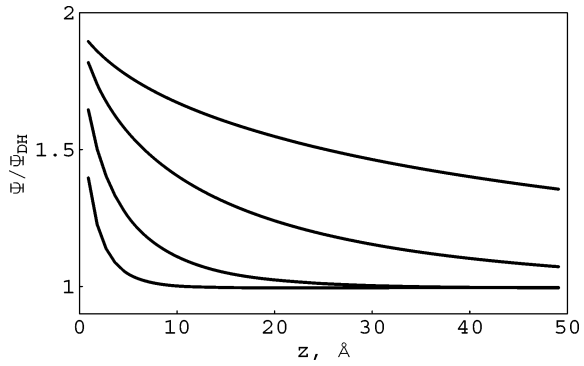

Figure 2. The electrostatic potential along the surface of a low-dielectric rod for the different values of the rod radius $a = 30$, 10, 3, and 1 Å (for the curves from top to bottom). Parameters: $\varphi = 0$, $\kappa^{-1} = 100$ Å; other parameters are the same as those in Figure 1.

In Figure 3, we also show the l_{tw}^{el} as obtained from the energy required to rotate a single base pair in the DNA structure (dashed curves). In this case, only the interactions between nearest charges along the same helical strand are counted for simplicity. We observe that for the values of twist angles β between the base pairs relevant to DNA, the l_{tw}^{el} is typically positive. As one could expect, the difference between the two values of twist PLs calculated from twisting the whole helix and from the twisting a single base pair becomes smaller at larger κ values when the interactions of far-apart charges is well

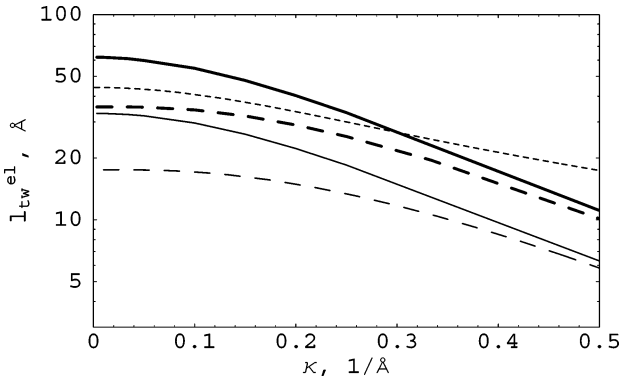

Figure 3. Characteristic length for the electrostatic twist rigidity as calculated for the DH (thin curves) and FS (solid curves) interactions between the charges on DNA. Dashed curves are the results of rotation of a single DNA base pair. The results of eqs 9 and 10 of ref 7 are shown as a dotted curve for the same parameters (with 15 terms counted in the sum). The parameters are the same as those in Figure 1, and $b = 3.4$ Å.

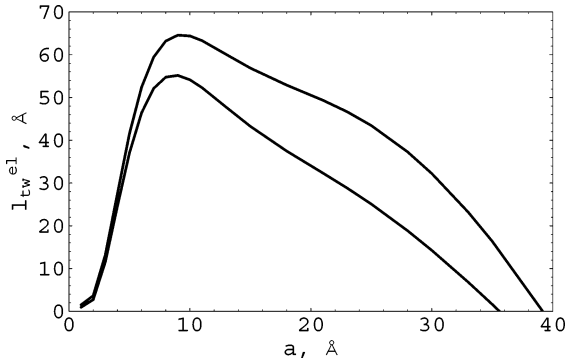

Figure 4. The same as in Figure 3 but for a low-dielectric rod as a function of the helix radius. Parameters: $\kappa^{-1} = 100$ Å (top curve) and 10 Å (bottom curve); other parameters and notations for the curves are the same as those in Figure 3.

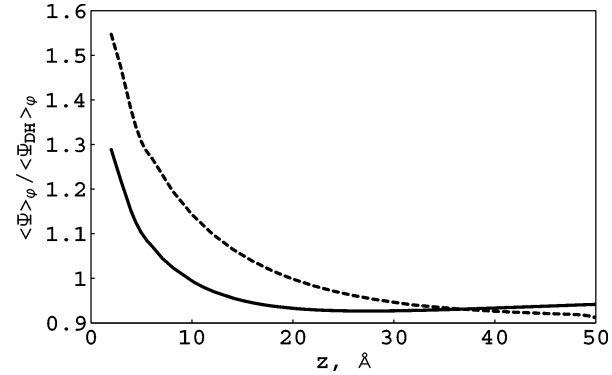

Figure 5. The ratio of the average FS and DH potentials for the interaction of charges along a rod for $\kappa^{-1} = 10$ Å (dotted curve) and 100 Å (solid curve). Other parameters are the same as those in Figure 1.

screened. This difference is due to the influence of the helical structure and charge−charge interactions across the rod. In Figure 3, we show also for comparison the results of ref 7, the dotted curve, which reveal a qualitative agreement with our numerical calculations. The l_{tw}^{el} reveals a non-monotonous dependence on the helix radius, Figure 4; see also Figures 5 and 7 of ref 7. We observe that at larger values of rod radius a and at a smaller κ, the landscape of E_{el} as a function of the twist rotation angle of a single base pair in the helix becomes more corrugated (as the charges separated by larger distances along the helix interact stronger).

3.2. Bending. Above, we have considered the ideal straight double helix that represents the positions of the phosphate charges of DNA. The large fraction of DNA is, however, known to be neutralized by the counterions adsorbed onto DNA from the bulk solution.[10] This cation's adsorption distorts, to some extent, the ideality of the helical pattern of the DNA phosphates considered above. The interaction of two changes in such a quasi-disordered distribution can be represented by a potential obtained via averaging of the interaction energy of two charges on the rod surface over the circumference position of the second charge, $\langle\Psi(\varphi,z)\rangle_\varphi$. This function thus characterizes the strength of charge−charge interactions along a straight low-dielectric quasi-uniformly charged rod. It should then be compared with the average DH potential

$$\langle\Psi_{DH}(\varphi,z)\rangle_\varphi = \frac{l_B}{2\pi}\int_0^{2\pi} d\varphi \frac{e^{-\kappa\sqrt{z^2+(2a\sin\varphi/2)^2}}}{\sqrt{z^2+(2a\sin\varphi/2)^2}} \qquad (5)$$

which would exist along a water-permeable rod.

For the parameters considered, the ratio of these two average potentials is larger than unity for small z values and levels off at larger z's, Figure 5. This function can be used to qualitatively predict the effects on l_p^{el} for a low-dielectric polyelectrolyte in the near-the-rod bending limit. We do not solve here the actual problem of the interaction of charges positioned in a helical manner on a bent arc of a low-dielectric rod. That is a rather complicated mathematical problem (see ref 6 for calculations of l_p^{el} for a water-permeable weakly bent helix). We however expect the electrostatic self-energy as well as the l_p^{el} for a low-dielectric rod to be larger than those for a high-dielectric water-filled rod because the dominant contributions come from the interactions of nearest charges along the rod, and they are substantially enhanced as compared to the DH results; see Figure 5. It would be interesting to study, in more detail in the future, the effects of charge discretization on the surface of polyelectrolytes with a low-dielectric core on their bending PL.

Above, we have considered the DNA molecule as an ideal double helix of charges. DNA helical parameters are however known to depend quite strongly on the DNA sequence, as the consideration of DNA crystals and DNA−protein complexes has shown; see refs 26, 27, and 28. Then, the following questions arise: (a) to what extent does the response of DNA to twisting and bending actually depend on the DNA sequence and (b) at which length scale are the effects of sequence specificity on twisting and bending averaged out for a genomic (or randomly sequenced) DNA? These questions are, however, beyond the scope of this paper. We hope that the effects of the low-dielectric molecular core on the DNA electrostatic persistence predicted here can be proved in the future on the basis of detailed computer simulations with more peculiarities of the DNA molecular structure being taken into account. They might include the structure of minor and major DNA grooves, the shell of structured water molecules near the DNA, the sequence-dependent DNA helical parameters, and a finite size of DNA charges.

Acknowledgment. I acknowledge the support by the Deutsche Forschungsgemeinschaft.

References and Notes

(1) (a) Odijk, T. *J. Polym. Sci.* **1977**, *15*, 477. (b) Fixman, M.; Skolnick, J. *Macromolecules* 1977, *10*, 944.

(2) Kunze, K. K.; Netz, R. R. *Phys. Rev. E* **2002**, *66*, 011918.

(3) Hagerman, P. J. *Biopolymers* **1983**, *22*, 811.
(4) Everaers, R.; Milchev, A.; Yamakov, V. *Eur. Phys. J. E* **2002**, *8*, 3, and references therein.
(5) Manning, G. S. *Biophys. J.* **2006**, *91*, 3607, and references therein.
(6) Manning, G. S. *Macromolecules* **2001**, *34*, 4650.
(7) Mohammad-Rafiee, F.; Golestanian, R. *Phys. Rev. E* **2004**, *69*, 061919.
(8) Cherstvy, A. G.; Winkler, R. G. *J. Phys. Chem. B* **2005**, *109*, 2962.
(9) Le Bret, M. *J. Chem. Phys.* **1982**, *76*, 6243.
(10) Manning, G. S. *Q. Rev. Biophys.* **1978**, *11*, 179.
(11) Hagerman, P. J. *Biopolymers* **1981**, *20*, 1503.
(12) Fixman, M. *J. Chem. Phys.* **1982**, *76*, 6346.
(13) Andreev, V. A.; Victorov, A. I. *Mol. Phys.* **2007**, *105*, 239.
(14) (a) Rouzina, I.; Bloomfield, V. A. *Biophys. J.* **1998**, *74*, 3152. (b) Ariel, G.; Andelman, D. *Europhys. Lett.* **2003**, *61*, 67.
(15) Fixman, M.; Skolnick, J. *Macromolecules* **1978**, *11*, 863.
(16) Netz, R. R. *Phys. Rev. E* **1999**, *60*, 3174.
(17) Cherstvy, A. G. *J. Phys. Chem. B* **2007**, *111*, 7914.
(18) Hoffmann, N.; Licos, C. N.; Hansen, J.-P. *Mol. Phys.* **2004**, *102*, 857.
(19) Allen, R.; Hansen, J.-P.; Melchionna, S. *Phys. Chem. Chem. Phys.* **2001**, *3*, 4177.
(20) Tanford, C. *Physical Chemistry of Macromolecules*; John Wiley: New York, 1961.
(21) Cherstvy, A. G.; Kornyshev, A. A.; Leikin, S. *J. Phys. Chem. B* **2002**, *106*, 13362, and references therein.
(22) Manning, G. S. *J. Phys. Chem. B* **2007**, *111*, 8554.
(23) Schurr, J. M.; Fujimoto, B. S. *Biophys. Chem.* **2002**, *101*−*102*, 425.
(24) Wilcoxon, J.; Schurr, J. M. *Biopolymers* **1983**, *22*, 2273.
(25) Schurr, J. M. *Biopolymers* **1985**, *24*, 1233.
(26) Olson, W.; Gorin, A.; Lu, X.; Hock, L.; Zhurkin, V. *Proc. Natl. Acad. Sci. U.S.A.* **1998**, *95*, 11163.
(27) Becker, N. B.; Wolff, L.; Everaers, R. *Nucl. Acid Res.* **2006**, *34*, 5638, and references therein.
(28) Cherstvy, A. G.; Kornyshev, A. A.; Leikin, S. *J. Phys. Chem. B* **2004**, *108*, 6508.